doi:10.2533/chimia.2009.193 Chimia 63 (2009) 193–196

Nickel Deposition on γ-Al_2O_3: Modelling Metal Particle Behaviour at the Support

Izabela Czekaj§*, Francois Loviat, Jörg Wambach, and Alexander Wokaun

§SCS Poster Prize Winner

Abstract: Recently, surface modifications on a commercial Ni/Al_2O_3 catalyst during the production of methane from synthesis gas were investigated by *quasi in situ* X-ray photoelectron spectroscopy (XPS). The effect of the synthesis gas on the surface properties of the catalyst and on its activity under methanation conditions was studied on an atomic level.[1] The conclusion was that the stability of Ni particles on the γ-Al_2O_3 support can be influenced by cluster growth phenomena, which influence both size and distribution of the metal particles. In this study, Ni deposition and cluster growth on model catalyst samples (10 nm thick, polycrystalline γ-Al_2O_3 on Si(100)) was investigated by XPS. The molecular structure of the catalyst was investigated using Density Functional Theory calculations (StoBe) with cluster model and non-local functional (RPBE) approach. $Al_{15}O_{40}H_{35}$ clusters were selected to represent the γ-Al_2O_3 (100) surface. Ni clusters of different size were cut from a Ni(100) surface and deposited on the $Al_{15}O_{40}H_{35}$ cluster in order to validate the deposition model determined by XPS.

Keywords: Alumina support · γ-Al_2O_3 · DFT · Methanation · Metal deposition · Metal–support interactions · Nickel catalyst · XPS

1. Introduction

Nickel-based catalysts supported on γ-Al_2O_3, TiO_2, Pt, zeolites or SiO_2,[2–9] are interesting examples due to their usage in numerous industrial processes.[2–5] Previously, it was shown that nickel particles change their morphology during catalytic reactions by cluster growth processes, and that part of the active clusters are lifted from the support due to carbon deposition and carbon whisker formation.[1] The industrial application of these types of catalysts[2,10] makes the investigation of the role of metal–support interactions for the Ni particle growth and detachment during methanation an important issue. Three different theoretical growth modes during metal deposition have been suggested:[6–9] 'Volmer-Weber' mode, where the deposited metal forms clusters immediately on the support; 'Frank van der Merwe' mode describes a layer-by-layer growth; and 'Stranski-Krastanov' mode, which includes a transition from an initial layer-by-layer to a consecutive three-dimensional cluster growth at a critical layer thickness. Some literature data[3,11–13] suggest the possibility that Ni ions migrate from the surface into the bulk forming nickel aluminate, $NiAl_2O_4$, where nickel appears in NiO form. The latter is extremely stable and difficult to reduce to metallic Ni, which is the catalytically active form. Ni^0 particles grow on top of the NiO interface later.[1]

Several theoretical investigations of the pure Ni system have been published[14–16] that focus on the stability and diffusivity of surface species, and further on possible mechanisms for the methane activation. Numerous theoretical studies on pure and modified γ-Al_2O_3 systems have been performed previously.[17–20] Theoretical investigations of the metal–support interactions for the adsorption of Pd on γ-Al_2O_3 have been published already.[21,22] However to our knowledge, theoretical studies about the combined Ni/γ-Al_2O_3 system are still missing in the literature.

In this paper, the results of a combined experimental and theoretical investigation on the Ni/γ-Al_2O_3 system are described. Emphasis was laid on understanding the Ni cluster growth and metal–support interactions. The goal was to define the geometry and favourable localization of metal particles on the support (disregarding steps or kink sites), metal–support interactions, chemical state of surface compounds, and the role of the support in the modification of the geometrical/electronic structure of metal particles and active sites. For the experiments, model catalysts were chosen due to the fact that they i) possess flat surfaces, which allow the application of AFM, SE, *etc.* and ii) allow a sufficient electron tunnelling through the (10 nm thin) γ-Al_2O_3 layer, making XPS and AES investigations possible.

2. Crystal Structure of Al_2O_3 and Nickel Clusters

The cubic phase[23,24] of defective alumina spinel, Al_2O_3, is described by the space group Fd-3m (a = b = c = 7.911 Å). Fig. 1 shows the structure of the γ-Al_2O_3(100) surface. Two different aluminium sites with four- and five-fold coordinated aluminium, AlO_4 and AlO_5, as well as two different three-fold coordinated oxygen sites, O(3) and O'(3), have been distinguished with Al–O distances of 1.94 Å and 1.78 Å. It is important to note that Al(4) is always located lower than the Al(5) centres and that the rows of AlO_5 pyramids are separated from each other by rows of AlO_4 tetrahedra. The (100) surface was chosen for our studies. The (100) surface exhibits specific holes with a distance of 2.90 Å and 2.79 Å between the O(3) centres. All these surface features are important, since sufficient compatibility of the (100) surface with the Ni particles is necessary in order to obtain stable Ni-clusters on the γ-Al_2O_3 support. Concerning the nickel particles,

*Correspondence: Dr. I. Czekaj
General Energy Research Department
Paul Scherrer Institut
CH-5232 Villigen PSI
Tel.: +41 56 310 4464
Fax: +41 56 310 2199
E-mail: izabela.czekaj@psi.ch

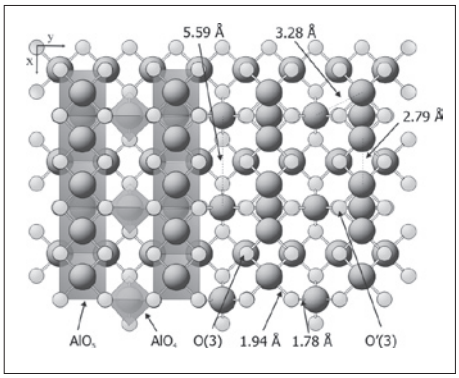

Fig. 1. Crystal structure of the γ-Al_2O_3(100) surface: top view with Al (large spheres) and O (small spheres). Note: the radii of the spheres do not correspond to the real radii. This is made for better visibility of active centres.

the cubic phase[25] of metallic nickel is described by the space group Fm-3m (a = b = c = 3.5239 Å). The distance between Ni–Ni is 2.49 Å.

3. Technical Details

3.1 *Experimental Details*

The XPS measurements were carried out in a VG Scientific ESCALAB 220i XL electron spectrometer. XPS measurements were made using non-monochromatic Mg Kα (1253.6 eV) radiation. During measurement, the chamber pressure was always lower than 1×10^{-9} Torr. The electron energy analyzer was operated in the constant-pass-energy mode with a pass energy of 50eV for survey scans and 20eV for detailed scans of selected spectral regions. The conductivity of the samples was high enough to keep sample charging below a few eV. For charge compensation, the binding energy (BE) scale was adjusted by setting the main C1s peak to 284.5eV. Quantification of the XP spectra was carried out using CasaXPS[26] and applying the transmission function of the electron energy analyzer and cross-sections calculated by Scofield. The spectra were deconvoluted by applying Gaussian-Lorentzian line-shapes with a Shirley-type background.

Attached *via* a distribution chamber is a preparation chamber equipped with a home-made metal evaporator. The evaporation rate was determined using a quartz micro balance. For a detailed description of the set-up see ref. [27]. The preparation chamber base pressure was less than 1×10^{-10} Torr, or during metal evaporation below 1×10^{-9} Torr. XPS characterisation was performed before and after any Ni evaporation and without exposure of the catalyst to air.

3.2 *Computational Details*

In our studies the Ni and γ-Al_2O_3 support surfaces are modelled by clusters of different size and geometry, which reflect local sections of the ideal surface. For the γ-Al_2O_3 cluster representing the support surface, formal valence charge saturation (based on Al^{3+}, O^{2-}) is imposed and cluster neutrality with respect to the surface is achieved by saturating by hydrogen (R_{OH} = 0.97Å). The thus obtained cluster $Al_{15}O_{40}H_{35}$ was selected for the investigation. Fig. 2a–c show the results of a geometric optimization of the chosen Ni clusters (Ni_2, Ni_7, Ni_9) on γ-Al_2O_3 cluster.

The electronic structure of all clusters was calculated by *ab initio* density functional theory (DFT) methods (program code StoBe[28]) using the non-local generalized gradient corrected functionals according to Perdew, Burke, and Ernzerhof (RPBE).[29,30] All Kohn-Sham orbitals are represented by linear combinations of atomic orbitals (LCAO's) using extended basis sets of contracted Gaussians from atom optimizations.[31,32] Detailed analyses of the electronic structure in the clusters are carried out using Mulliken populations[33] and Mayer bond order indices.[34,35] During relaxation, the nickel atoms in the supported clusters were allowed to move in 3D space.

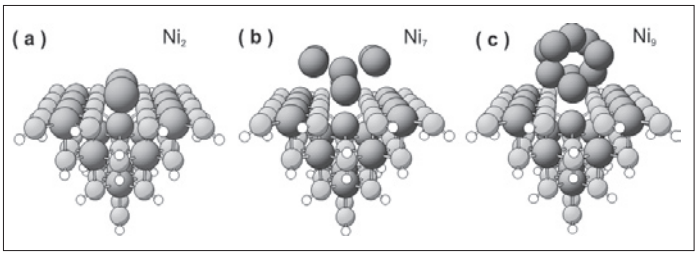

Fig. 2. Models of Ni clusters: relaxed on the γ-Al_2O_3(100) surface represented by $Al_{15}O_{40}H_{35}$ cluster: (b) Ni_2 cluster, (c) Ni_7 cluster, (d) Ni_9 cluster.

4. Results

4.1 *XPS Results of Ni Deposition at Al_2O_3: The Role of Deposition Time with Regard to Changes in the Chemical State of Surface*

Fig. 3a gives the Ni $2p_{3/2}$/Al 2p ratio versus the deposition (expressed in seconds) of nickel onto the γ-Al_2O_3 support. Experimentally obtained data are represented by dots. The deposition was performed with a deposition rate corresponding (theoretically) to 0.75 ML/min. The solid line symbolizes the theoretically expected Ni $2p_{3/2}$/Al 2p ratio for a pure layer-by-layer growth. For this estimation, we presumed that this (theoretical) Ni monolayer would

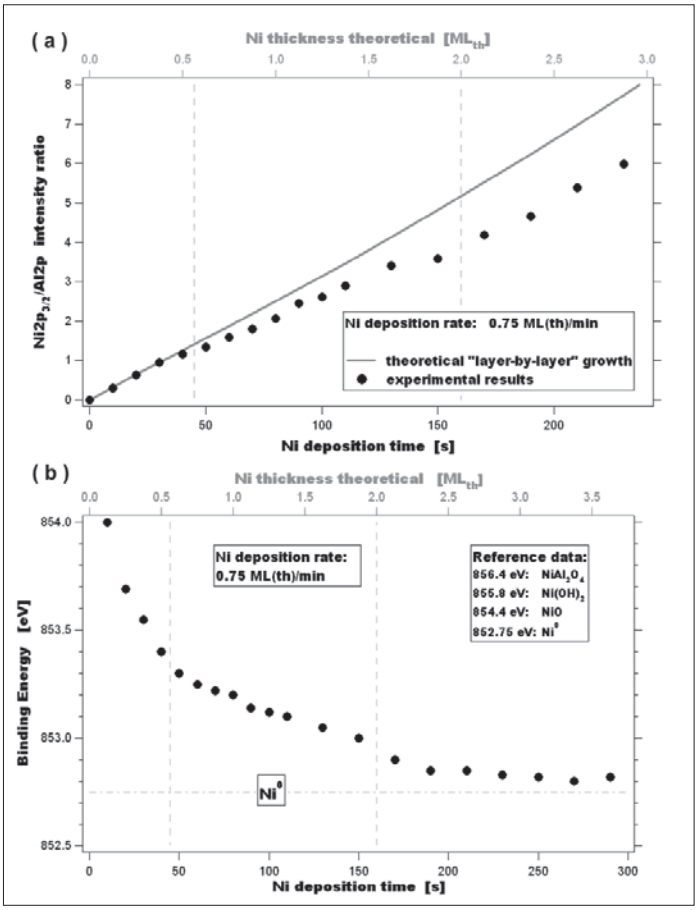

Fig. 3. Changes of: (a) Ni $2p_{3/2}$/Al 2p ratio during deposition of nickel onto the Al_2O_3 support. (The solid line corresponds to the theoretical prediction of the Ni $2p_{3/2}$/Al 2p ratio for a layer-by-layer growth. The theoretical depositions times for 0.5 ML and 1.0 ML of Ni (layer-by-layer growth) are indicated, too.) (b) XPS Binding Energies of the Ni $2p_{3/2}$ peak during deposition of nickel on γ-Al_2O_3. – The inset gives binding energy data[37] for different Ni compounds as reference.

have the dense geometry of a Ni(100) monolayer on the γ-Al_2O_3. Up to a deposition time t ~ 45 s, our experimental data follow almost the expected layer-by-layer growth line. This suggests that in the initial phase Ni does not form clusters immediately, but 1D (or possibly 2D) agglomerates. In a second stage, the Ni $2p_{3/2}$/Al 2s ratio is below the 'layer-by-layer' line. This makes it likely that in this phase 3D Ni clusters are growing on the surface. We conclude that Ni deposition on γ-Al_2O_3 support follows a kind of 'modified' Stranski-Krastanov growth mode under the applied experimental conditions, which is in accordance with the findings of Jacobs *et al.*[4]

A support for the suggested change in the growth mode can be found by the change of the binding energy (BE) (Fig. 3b). The change of the binding energy can be separated into three parts, as indicated by the two vertical lines. In the initial part, the very first Ni atoms exhibit a BE value of *ca* 854.0 eV, which is close to published Ni oxide (NiO) data.[12,13,36,37] This can be interpreted as single Ni atoms being deposited and chemically modified by being bonded strongly to the oxygen of the support. The further initial part up to about 45 s is characterised by a fast decrease of the BE down to *ca* 853.3 eV. In the second part, between 50 s and about 150 s deposition times, the slope of the BE change is decreased and the BE value is lowered to 853.0 eV. The final part, *i.e.* deposition times more than 170 s, is characterised by a slow approach to 852.75 eV (obtained for deposition times >350 s (not shown)), the value of metallic Ni as indicated by the horizontal dash-dotted line.

Interestingly, the time of the transition from the first to the second part (~45 s) is comparable with the time where the deviation of the experimentally derived Ni $2p_{3/2}$/Al 2p ratio from the 'layer-by-layer' ratio starts, as shown in Fig. 3a (see the vertical line). This makes it likely that in this stage additional Ni atoms are added to the already existing ones forming 3D-Ni agglomerates. These Ni agglomerates are still not metallic, but 'chemically modified'. The third part indicates that continual cluster growth produces 3D-Ni clusters, which finally from a band structure typical for bulk Ni.

4.2 *DFT Modelling of the Ni/Al_2O_3 Interface*

The Table presents information about atomic charges (Mulliken analysis), distances (Å) and bond orders (Mayer bond analysis) of clusters $Al_{15}O_{40}H_{35}$ and Ni_x/$Al_{15}O_{40}H_{35}$ (x = 2,7,9). The data are basing on optimisation calculations described in Section 3.2. The charge of aluminium centres on the (100) surface increases in the order q[Al(5)] < q[Al(6)] < q[Al(4)]. The Al(5) centre is stronger bound to the surface (Σb.o.=3.1) than Al(4) (Σb.o.=2.3), but is not fully coordinated. Therefore, the Al(5) centre can be easily oxidized or hydrated.

Table. Results obtained by DFT calculations summarising atomic charges (eV), distances (Å) and bond orders (Mayer bond analysis) of (a) the $Al_{15}O_{40}H_{35}$ cluster, (b) the Ni_2 at Al_2O_3 cluster, (c) the Ni_7 at Al_2O_3 cluster, and (d) the Ni_9 at Al_2O_3 cluster.

		(a)	(b)	(c)	(d)
Cluster:		$Al_{15}O_{40}H_{35}$	Ni_2 / $Al_{15}O_{40}H_{35}$	Ni_7 / $Al_{15}O_{40}H_{35}$	Ni_9 / $Al_{15}O_{40}H_{35}$
Centre		Charge [eV]			
Al(4)		+1.58	+1.87	+2.20	+2.16
Al(5)/Al(6)		+0.99/+1.11	+0.91/+1.13	+0.80/+1.13	+1.01/+1.15
O(3)		–0.68	–0.82	–0.89	–0.92
O`(3)		–0.75	–0.78	–0.84	–0.89
Ni^{1st}		–	+0.28	+0.38	+0.35
Bond	Distance [Å]	Bond Order			
O(3)-Al(5)	1.94/1.94	0.73/0.66	0.61/0.58	0.66/0.45	0.66/0.51
O(3)-Ni	(see diff. Ni_x)	–	0.21 (2.16Å)	0.17 (2.04Å)	0.15 (2.09Å)
O'(3)-Al(5)	1.94/1.94	0.66/0.66	0.61/0.61	0.58/0.58	0.57/0.55
O'(3)-Al(4)	1.78	0.63	0.43	0.48	0.38
O'(3)-Ni	(see diff. Ni_x)	–	0.08 (2.57 Å)	0.01 (2.96 Å)	0.004 (3.10Å)
Ni^{1st}-Ni^{1st}	(see diff. Ni_x)	–	0.34 (3.53 Å)	0.08 (4.52 Å)	0.09 (4.77 Å)

The two types of surface three-coordinated oxygen centres, O(3) and O'(3), are similarly bound to the surface (Σb.o.~2.0), but show a different ionic character. The O'(3) centres, connected with five- and four-coordinated aluminium centres, have higher charge and should be more reactive than O(3).

The $Al_{15}O_{40}H_{35}$ cluster was found to be a good representation for the electronic states of both oxygen O'(3) and O(3) as well as three types of aluminium centres, Al(4), Al(5) and Al(6), present on the Al_2O_3(100) surface. Taking into account computational time (including optimization and metal deposition at the surface) as well as accuracy of the electronic structure, the $Al_{15}O_{40}H_{35}$ cluster seems to be a good enough compromise of cluster convergence criteria and therefore was chosen for all further considerations in metal deposition studies.

The stabilization energy of nickel particles deposition on $Al_{15}O_{40}H_{35}$ cluster is calculated as the difference between the total energy of the metal deposited at the Al_2O_3 surface and sum of the total energies of pure $Al_{15}O_{40}H_{35}$ and the M atoms, respectively. In all cases, the first layer of nickel deposits on the Al_2O_3(100) in positions closer to O(3) centres with different stabilization energy per Ni atom (for Ni_2: –0.82eV, for Ni_7: –0.90eV and for Ni_9: –0.71eV). The determined stabilization energies of the different Ni clusters are in the range obtained for the adsorption of different metals, mainly Pd, on γ-Al_2O_3.[19,20] The deposited nickel influences the electronic structure of γ-Al_2O_3 and is strongly bound to octahedral O(3).

The largest investigated nickel cluster (Ni_9) creates many interesting structures at the support surface. Fig. 4 shows the interface atoms of the Ni_9 cluster after relaxation. The figure was created by multiplying the calculated Ni/Al_2O_3 cluster in x and y direction. The black dots, added for comparison with the relaxed structure, symbolize the mismatch of an 'ideal' Ni(100) monolayer with the γ-Al_2O_3 surface. Dark-gray spheres give the positions of Ni atoms with coverage θ ~ 0.40 ML. Strong vertical and lateral re-arrangements of the interface Ni atoms in the Ni_9 clusters with respect to the position on the Ni(100) surface are indicated by our DFT results. Part of the nickel atoms seem to prefer the 'valley regions' between AlO_5 rows and close to O(3) centres. After deposition of a very low number of metal atoms on γ-Al_2O_3, only the local surface structure is influenced, in particular the neighbouring centres of Ni, such as: Al(4), Al(5), O(3) and O'(3). The O(3) centres are mostly influenced creating strong bonds with the first (interface layer) nickel atoms. This finding is in good accordance with our experimental results (see Fig. 3b), where we observe the existence of electronically strongly altered Ni being adsorbed on γ-Al_2O_3 in the first stage of the deposition. As mentioned above, we presume that initially single Ni atoms are deposited, and that consecutive Ni deposition (up to ~45 s) leads to the formation of either 1D-Ni chains or 2D-Ni agglomerates.

A further important question is the suggested existence of nickel aluminate in the interface and its influence on cluster stabil-

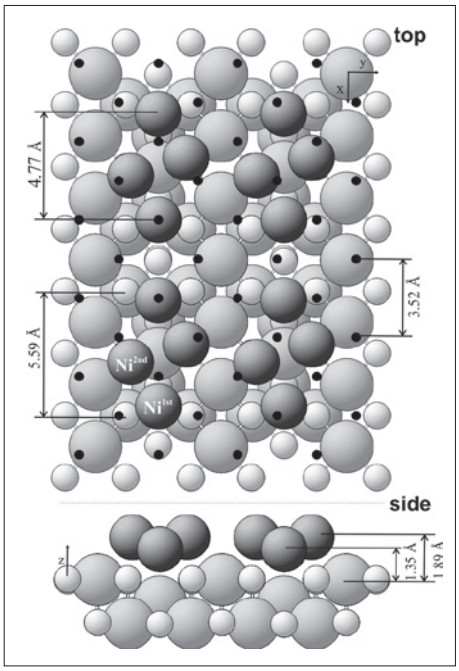

Fig. 4. Topography (top and side view) of first (interface) Ni atoms (dark-gray spheres) for the relaxed Ni_9 cluster from an $Al_{15}O_{40}H_{35}$ cluster: all Ni interface atoms included (θ_{Ni} ~ 0.4 ML). Black dots symbolize the position of Ni atoms in an ideal Ni(100) monolayer.

ity at alumina. Studies going in that direction are presently running in our laboratory and will be presented elsewhere.[38]

5. Conclusions

Nickel is stabilized on the γ-Al_2O_3 surface influencing the electronic properties of the newly formed surface. Our DFT data suggest that at low coverages (≤ 0.2 ML) Ni prefers being localized in AlO_4 tetrahedra between rows of AlO_5. The DFT results correspond well with the experimental data of the initial stage of Ni deposition, where the formation of a partial Ni monolayer is suggested. Additional Ni deposition leads first to non-metallic three-dimensional agglomerates, which are finally transferred to metallic Ni clusters on the surface by continual Ni deposition. For Ni_7 and Ni_9 clusters, the initially deposited Ni atoms, which represent the interface nickel atoms ('Ni^{1st}'), are bound strongly to the oxygen of the support and are located in positions closer to O(3) centres as well as between rows of AlO_5 with adsorption energy, which varies with the size of the cluster.

Acknowledgement

The calculations were done partially using the unix farm as well as the linux farm at the Paul Scherrer Institut. We would like to express our thanks to M. Horisberger for preparation of the γ-alumina model support.

Received: December 19, 2008

[1] I. Czekaj, F. Loviat, F. Raimondi, J. Wambach, S. Biollaz, A. Wokaun, *Appl. Catal. A* **2007**, *329*, 68.
[2] G. Ertl, H. Knözinger, J. Weitkamp, 'Handbook of Heterogeneous Catalysis', Wiley, Weinheim, **1997**.
[3] D. Nazimek, A. Machocki, T. Borowiecki, *Adsorp. Sci. Technol.* **1998**, *16*, 747.
[4] J. P. Jacobs, L. P. Lindfors, J. G. H. Reintjes, O. Jylhä, H. H. Brongersma, *Catal. Lett*. **1994**, *25*, 315.
[5] T. J. Sarapatka, *Chem. Phys. Lett.* **1993**, *212*, 37.
[6] C. S. Shern, J. S. Tsay, T. Fu, *Appl. Surf. Sci.* **1996**, *92*, 74.
[7] R. E. Tanner, I. Goldfarb, M. R. Castell, G. A. D. Briggs, *Surf. Sci.* **2001**, *486*, 167.
[8] J. D. Carey, L. L. Ong, S. R. P Silva, *Nanotechnol.* **2003**, *14*, 1223.
[9] M. A. Karolewski, *Surf. Sci*. **2002**, *517*, 138.
[10] M. C. Seemann, T. J. Schildhauer, S. M. A. Biollaz, S. Stucki, A. Wokaun, *Appl. Catal. A* **2006**, *313*, 14.
[11] R. Lamber, G. Schulz-Ekloff, *Surf. Sci.* **1991**, *258*, 107.
[12] K. Shih, J. O. Leckie, *J. Euro. Ceramic Soc.* **2007**, *27*, 91.
[13] R. Lamber, G. Schulz-Ekloff, *Surf. Sci.* **1991**, *258*, A595.
[14] J. Sehested, J. A. P. Gelten, I. N. Remediakis, H. Bengaard, J. K. Nørskov, *J. Catal.* **2004**, *223*, 432.
[15] H. S. Bengaard, J. Nørskov, J. Sehested, B. S. Clausen, L. P. Nielsen, A. M. Molenbroek, J. R. Rostrup-Nielsen, *J. Catal.* **2002**, *209*, 365.
[16] F. Abild-Pedersen, O. Lytken, J. Engbaek, G. Nielsen, I. Chorkendorff, J. K. Nørskov, *Surf. Sci*. **2005**, *590*, 127.
[17] J. Handzlik, J. Ogonowski, R. Tokarz-Sobieraj, *Catal. Today* **2005**, *101*, 163.
[18] M. Digne, P. Sautet, P. Raybaud, P. Euzen, H. Toulhoat, *J. Catal.* **2004**, *226*, 54.
[19] A. Ionescu, A. Allouche, J. P. Aycard, M. Rajzmann, F. Hutschka, *J. Phys. Chem. B* **2002**, *106*, 9359.
[20] C. Arrouvel, M. Breysse, H. Toulhoat, P. Raybaud, *J. Catal.* **2005**, *232*, 161.
[21] A. M. Marquez, J. F. Sanz, *Appl. Surf. Sci*. **2004**, *238*, 82.
[22] M. C. Valero, P. Raybaud, P. Sautet, *J. Phys. Chem. B* **2006**, *110*, 1759.
[23] R.-S. Zhou, R. L. Snyder, *Acta Cryst. B* **1991**, *47*, 617.
[24] E. J. W. Verwey, *Z. Krist.* **1935**, *91*, 317.
[25] R. W. G. Wyckoff, 'Crystal Structures', Interscience Publishers, John Wiley & Sons, Inc., New York - London - Sydney, Vol. I, **1965**.
[26] N. Fairley, CasaXPS Software, Version 2.3.12, **2006**.
[27] F. Loviat, PhD thesis, 'Photoassisted activation of methane with a xenon excimer lamp', ETH, **2008**.
[28] The program package StoBe is a modified version of the DFT-LCGTO program package DeMon, originally developed by A. St.-Amant and D. Salahub (University of Montreal), with extensions by L. G. M. Pettersson and K. Hermann.
[29] J. P. Perdew, K. Burke, M. Ernzerhof, *Phys. Rev. Lett.* **1996**, *77*, 3865.
[30] B. Hammer, L. B. Hansen, J. K. Nørskov, *Phys. Rev. B* **1999**, *59*, 7413.
[31] 'Density Functional Methods in Chemistry', Ed. J. K. Labanowski, J. W. Anzelm, Springer -Verlag, New York, **1991**.
[32] N. Godbout, D. R. Salahub, J. Andzelm, E. Wimmer, *Can. J. Phys*. **1992**, *70*, 560.
[33] R. S. Mulliken, *J. Chem. Phys.* **1955**, *23*, 1833, 1841, 2388, 2343.
[34] I. Mayer, *Chem. Phys. Lett.* **1983**, *97*, 270.
[35] I. Mayer, *J. Mol. Struct. (Theochem)* **1987**, *34*, 81.
[36] 'Handbook of X-ray Photoelectron Spectroscopy', Ed. J. F. Moulder, W. F. Stickle, P. E. Sobol, K. D. Bomben, J. Chastain, Perkin-Elmer Corporation, Physical Electronics Division, Eden Prairie, Minnesota, USA, **1992**.
[37] C. D. Wagner, A. V. Naumkin, A. Kraut-Vass, J. W. Allison, Cedric J. Powell, J. R. Rumble Jr., NIST X-ray Photoelectron Spectroscopy Database, NIST Standard Reference Database 20, Version 3.4 (Web Version), National Institute of Standards and Technology, Gaithersburg, USA, **2006**.
[38] I. Czekaj, J. Wambach, A. Wokaun, to be published.